IEEE Access
Multidisciplinary | Rapid Review | Open Access Journal

Received 25 April 2024, accepted 15 May 2024, date of publication 21 May 2024, date of current version 30 May 2024.

Digital Object Identifier 10.1109/ACCESS.2024.3403717

RESEARCH ARTICLE

On-Line Measurement Method for Rheology of Straight Tubular Oil-Based Drilling Fluid Under Pulsating Flow

XUEQIANG WANG[1], YILIN CHEN[1], WEN ZHANG[1], JI ZHANG[1], YIN LEI[1], DONGXU TU[1], HANG LU[1], KE YAN[2], GUOYONG XIA[3], HAOSEN YUAN[1], HAN ZHANG[1], AND YU XU[1]

[1]Engineering Technology Research Institute, PetroChina Southwest Oil and Gas Field Company, Chengdu 610000, China
[2]Exploration Division, PetroChina Southwest Oil and Gas Field Company, Chengdu 610041, China
[3]Development Division, PetroChina Southwest Oil and Gas Field Company, Chengdu 610051, China

Corresponding author: Yilin Chen (chenyilin_CNPC@163.com)

This work was supported by the Scientific Research Start-Up Project of PetroChina Southwest Oil and Gas Field Branch under Grant 2021030226.

ABSTRACT With the rapid development of drilling automation, how to automate real-time online measure drilling fluid rheology accurately has become one of the problems that the industry urgently wants to solve. At present, the common method is the rheological measurement method of straight pipe drilling fluid, but often the pumping equipment will produce pulsating flow during reciprocating pumping, resulting in a large error in the data of pressure difference and flow measurement, and the corresponding rheological parameters obtained are not accurate. In order to solve the problem of low accuracy of rheological parameters, this paper proposes an online measurement method for the rheology of straight tubular oil-based drilling fluids under pulsating flow, and firstly establishes an online measurement model of the rheology of straight tubular oil-based drilling fluids. Then, fluent is used to simulate and analyze the fluid movement of drilling fluid with different rheology in the measuring tube, and then analyze the error of differential pressure measurement and flow measurement of the measuring tube under the fluctuating flow. The actual measurement environment was simulated as the initialization parameters of the fluent simulation, and the calibration model of the oil-based drilling fluid measured by the device under the influence of pulsation was established. Finally, the experimental bench was built, and the experimental results showed that the calculated rheological parameters were 2.69% for apparent viscosity (AV), 2.362% for plastic viscosity (PV) and 3.056% for yield point (YP), which effectively improved the online measurement accuracy of straight tube oil-based drilling fluid.

INDEX TERMS Drilling fluid rheology, straight tube measurement, pulsating flow, fluent simulation analysis, fluid measurement models.

I. INTRODUCTION

Oil-based drilling fluid has many advantages, such as high temperature resistance, salt and calcium ingress resistance, good wellbore stability, good lubricity and less damage to oil and gas reservoirs. Oil-based drilling fluid has become an important means of drilling difficult high-temperature deep wells, high-inclination directional wells, horizontal wells and various complex formations, and can also be widely used as decard fluid, perforation and completion fluid, workover fluid and coring fluid. Therefore, real-time online measurement of the rheology of oil-based drilling fluids is necessary [1]. In terms of the process of drilling automation, the current measurement method mainly relies on manual measurement, in which the measurement process needs to collect samples, transport, process and analyze the measurement data before the measurement results can be obtained [2], [3]. The disadvantage of this measurement method is that it is not possible to analyze the problems and effects of the drilling process in real time [4]. In the strict on-site environment of the drilling

The associate editor coordinating the review of this manuscript and approving it for publication was Fabrizio Messina.

site, strict standards are put forward for the monitoring of the rheological performance of drilling fluids, that is, the drilling fluid must complete the tasks of suspension, pressure control, bare rock stability, buoyancy, lubrication and cooling, etc., and the inability to quickly and accurately monitor the rheology of drilling fluid has restricted the pace of optimizing the drilling progress [5].

There have been some researches on automatic rheological measurement of drilling fluid. Saasen A. et al. added a speed regulating mechanism to the rotational viscometer to realize the automatic measurement of drilling fluid rheology, but it takes a long time to achieve a stable state of the fluid during the measurement process. The real-time nature of this measurement process is poor [6]. Halliburton has developed a fully automated BaraLogix DRU mud rheometer based on the tubular measurement method, an accessory that draws drilling fluids from a pool and circulates them over a small area, without considering the effect of fluid pulsation on measurement accuracy.

At present, the common automatic measurement method is the straight tube rheology measurement, but when this method is used, it needs pumping equipment to extract the measurement sample into the pipeline [7], [8]. The pumping equipment selected in the tube measurement is generally a plunger pump and a diaphragm pump [9]. Diaphragm pump and plunger pump are both reciprocating positive displacement pumps, and the fluctuation caused by the reciprocating movement of the two pumps can change the flow field in the tube and form a fluid pulsating flow [4], [10]. However, the linear tube measurement method takes the flow rate inside the pipe segment and the pressure difference between the two ends as the central measurement parameters, and the fluid pulsation seriously interferes with the measurement accuracy of the linear tube, making the measurement error accuracy generally greater than 10%, which affects the measurement accuracy of the linear tube under the influence of fluid pulsation [11], [12].

In view of the processing of fluid pulsating flow, some scholars have done some research in this aspect. Lee et al. carried out finite element simulation analysis of the diaphragm head seal structure of the diaphragm pump through modeling, and the results obtained by the simulation software were the results under the static condition, so they were very different from the actual dynamic conditions [13]. Mi et al. carried out simulation experiments to verify the pulsation of the peristaltic diaphragm pump through dynamic modeling, but did not actually build an experimental platform for experimental verification under the same conditions, so whether it is accurate remains to be verified [9]. Fei et al. analyzed the piston chamber pumped by the diaphragm pump and optimized the design and strengthened the structure, but the effect achieved was unsatisfactory, and it could only work on pulsation at a specific pulsation frequency [14].

In view of the above problems of low accuracy of automatic rheological measurement of drilling fluid and the influence of fluid pulsating flow, this paper proposes an online measurement method for the rheological measurement of oil-based drilling fluid in a straight pipe under pulsating flow. First, an online measurement model for the rheological measurement of oil-based drilling fluid in a straight pipe is established. Then, fluent was used to simulate the movement of drilling fluid with different rheological properties in the measuring tube, and the error of pressure difference measurement and flow measurement in the pulsating flow tube was analyzed. The actual measurement environment was simulated as the simulation initialization parameter of fluent, and the calibration model of the measurement of oil-based drilling fluid under the influence of pulsation was established.

II. RESEARCH ON ON-LINE MEASURING METHOD OF RHEOLOGY OF STRAIGHT TUBE

A. ESTABLISHMENT OF ON-LINE MEASURING MODEL FOR RHEOLOGICAL PROPERTIES OF OIL-BASE DRILLING FLUID WITH STRAIGHT PIPE

The rheological measurement of drilling fluid in straight pipe is to measure the pressure difference data and the corresponding flow rate under different flow rates in a measuring straight pipe of known size, calculate the corresponding wall shear rate and stress, and draw the rheological curve, and finally obtain the specific rheological parameter values according to the rheological curve [15], [16].

As shown in Figure 1, drilling fluid samples are pumped from the mud pool into the measuring straight pipe by pumping equipment, and then flow back to the mud tank after measuring. Mass flowmeter measures flow; The two probes of the differential pressure sensor are installed at both ends of the measuring straight pipe to measure the differential pressure of the pipe segment; Then by setting the working voltage of the pumping equipment according to the gradient change, different flow rate and pressure difference measurement values are obtained. Then, the rheological curve of drilling fluid is calculated and plotted according to these measurement data, and the rheological parameters of oil-based drilling fluid can be measured online.

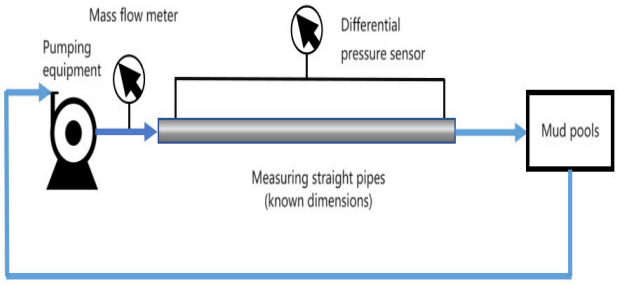

FIGURE 1. Schematic diagram of the principle of straight tube measurement.

In the process of straight tube rheology measurement, the differential pressure and flow rate are the data used to solve the rheological parameters of the drilling fluid [17], [18]. To obtain the rheological parameters of drilling fluid, it is necessary to draw the rheological curves of the wall shear

rate and the wall shear stress, and the calculation flow chart is shown in Figure 2.

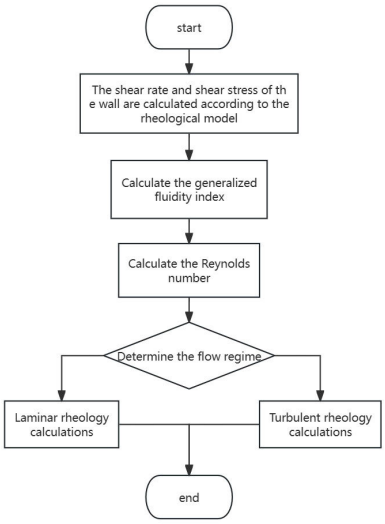

FIGURE 2. Flow chart of rheological parameter calculation.

(1) When the fluid in the straight pipe moves in steady state

According to the principle of force balance in the straight pipe, one is the force $F1$ acting on the pipe wall at both ends of the straight pipe ΔP, and the other is the viscous resistance $F2$ when the fluid flows on the wall. Let r be any distance point between the inner center point of the pipe and the pipe wall, and R be the inner radius of the pipe. Thus, in laminar flow, we can obtain the formula of shear stress on the wall,

$$\pi r^2 \cdot \Delta P - 2\pi rL\tau = 0 \tag{1}$$

$$\tau = \frac{\Delta P}{2L} \tag{2}$$

where, τ – shear stress on straight pipe wall (Pa).

At r=R, τ is the largest, the fluid resistance is the largest, and the flow rate is 0. At the center of the tube, at r=0, τ is the smallest, the resistance is the least, and the flow rate is the largest. Finally,

$$\frac{\tau}{\tau_B} = \frac{r}{R} \tag{3}$$

The above two formulas are applicable to any time-independent fluid in steady state flow.

(2) The flow characteristics of Newton fluid pipe flow can be obtained by sorting out Hagen's equation

$$Q = \frac{\Delta P \cdot \pi R^4}{8\mu L} \tag{4}$$

And $Q = \pi D^2/4$, it get,

$$\tau_B = \mu \frac{8v}{D} \tag{5}$$

According to Newton's equation, since $\tau_R = \mu\left(-\frac{dv}{dr}\right)$, therefore $-\frac{dv}{dr} = \frac{8v}{D}$.

(3) Pipe flow characteristics of non-Newtonian fluids

In order to obtain the rheological curve of a non-Newtonian fluid and determine its rheological properties, it is necessary to know the shear stress τ_B and shear rate $\left(-\frac{dv}{dr}\right)$ when the pipe flow is flowing. Suppose $y=v$, then $dy = dv$; $z = \pi r^2$, $dz = 2\pi rdr$,the integral arrangement gives like this,

$$\int_a^b ydz = yz|_a^b - \int_a^b zdy \tag{6}$$

When $r=R$ and flow rate $v=0$, the arrangement is as follows,

$$Q = \int_0^R \pi r^2 \left(-\frac{dv}{dr}\right) dr \tag{7}$$

According to $Q = v\pi R^2 = \frac{v\pi D^2}{4}$, $R = \frac{D}{2}$.The collation and simplification is as follows,

$$\frac{8v}{D} = \frac{32}{D^3} \int_0^{D/2} r^2 \left(-\frac{dv}{dr}\right) dr \tag{8}$$

Shear rate and shear stress can be expressed by $\left(-\frac{dv}{dr}\right) = f(\tau)$,According to the formula (3-3), can be obtained $dr = \frac{D}{2\tau_B} d\tau$,

$$\frac{8v}{D} = \frac{4}{(\tau_B)^3} \tau \int_0^{\tau_B} \tau^2 f(\tau) d \tag{9}$$

$$Q = \frac{\pi R^3}{(\tau_B)^3} \int_0^{\tau} B\tau^2 f(\tau)\, d\tau \tag{10}$$

The non-Newtonian fluid $\frac{8v}{D}$ has a certain functional relationship with the shear stress of the pipe wall, so $\frac{8v}{D} = \phi(\tau_B)$ is assumed,

$$4f(\tau_B) = 3\phi(\tau_B) + \frac{\tau_B}{d\tau_B} \cdot d\tau_B \cdot \frac{\phi'(\tau_B)}{\phi(\tau_B)} \cdot \phi(\tau_B) \tag{11}$$

On account of $\frac{d\tau_B}{\tau_B} = d\ln\tau_B$, $\frac{\phi'(\tau_B)}{\phi(\tau_B)} = d\tau_B$,The generalized fluidity index $\frac{d\ln\tau_B}{d\ln(8v/D)} = N$can be obtained,

$$4\left(-\frac{dv}{dr}\right) = 3\left(\frac{8v}{D}\right) + \frac{d\ln(8v/D)}{d\ln\tau_B} \cdot \frac{8v}{D} \tag{12}$$

Therefore, by substituting $\frac{d\ln(8v/D)}{d\ln\tau_B} = \frac{1}{N}$, the wall shear rate can be obtained as,

$$\left(-\frac{dv}{dr}\right) = \gamma = \frac{8v}{D}\left(\frac{3N+1}{4N}\right) \tag{13}$$

The above equation (13) is a shear rate calculation model for time-independent non-Newtonian fluids (including Newtonian fluids) at the tube wall.

B. DESIGN OF LINEAR RHEOLOGICAL MEASUREMENT SCHEME

The rheological parameters such as plastic viscosity, apparent viscosity and dynamic shear force can be measured and calculated in real time by using the differential pressure sensor installed at both ends of the measuring tube and combining the parameters of drilling fluid density, temperature and mass flow measured by the mass flowmeter.

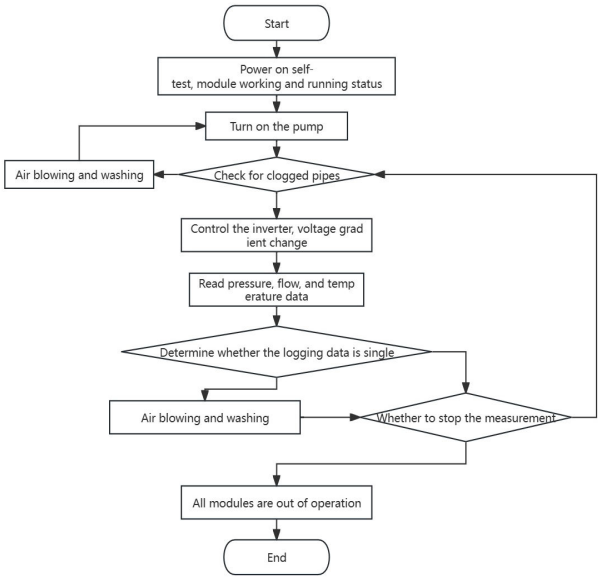

FIGURE 3. Control flow chart.

The control flow chart is shown in Figure 3.

A certain volume of drilling fluid is extracted from the mud tank into the measurement pipeline by controlling the driving voltage value of the electric diaphragm pump (adjustable speed and kept constant), and pulsating flow with different frequency and pulsating amplitude is generated into the measurement system by controlling the diaphragm pump. Then the measurement data value of each measurement component is transmitted to the host computer through the communication protocol. Finally, the upper computer software calculates and outputs the measured value, and finally returns to the mud tank.

III. LINEAR TUBE FLUID KINEMATICS ANALYSIS

FLUENT in Ansys was used to simulate and analyze the fluid movement of drilling fluid with different rheology in the measuring tube, so as to observe the impact of pulsating flow and measuring pressure difference with different rheology under normal conditions. The simulation flowchart is shown in Figure 4,

A. SIMULATION OF MEASURING TUBES WITHOUT PULSATION

The measuring tube model is made of 316L stainless steel with a measuring tube length of 1300mm and a tube diameter of 25mm. The pipeline model is shown below,

According to the size of the pipeline, the fluid flow area is divided into grids, as shown in the figure below,

The boundary conditions should be given to determine the accuracy and convergence of the calculation model when the pipeline drilling fluid flow field is analyzed. There are mainly import boundary conditions and export boundary conditions. Inlet flow rate was calculated by flow rate and pipe diameter. Rheological form of drilling fluid adopted

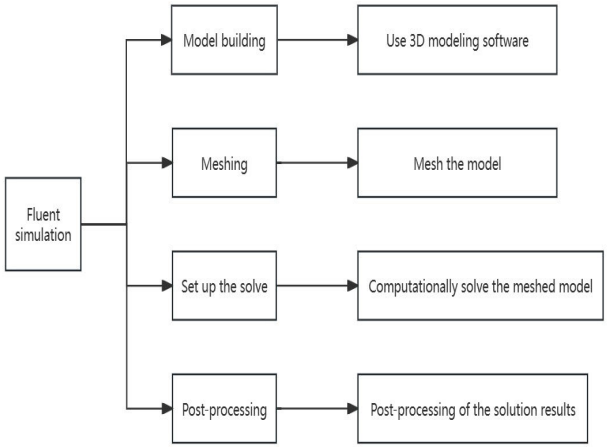

FIGURE 4. Fluent simulation flow chart.

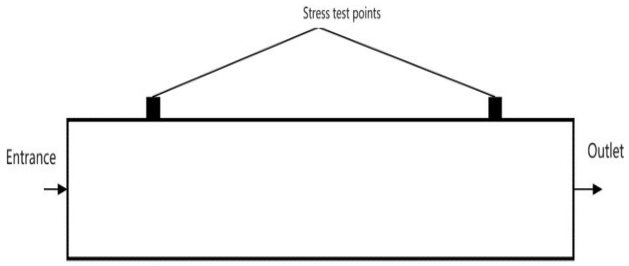

FIGURE 5. Pipeline model diagram.

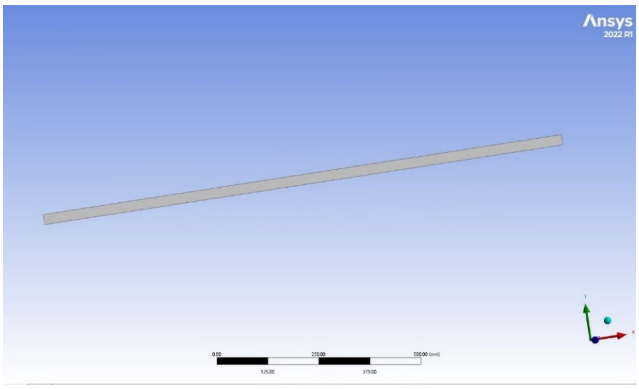

FIGURE 6. 2D model drawing of measuring tube.

laminar flow. Outlet boundary conditions mainly included outlet diameter and pressure outlet, and the parameter was set to 0Mpa. Then, other initial parameters were set. Elasticity model E=208GPa, Poisson's ratio, considering gravity, Y-axis $-9.8 m/s^2$, flow rate 0.8m/s, fluid density $1100 kg/m^3$, and SSTk-omega turbulence model were adopted. After setting, 1000 steps of iteration is set as the upper limit for calculation, and the simulated static pressure cloud image is obtained as shown in the figure,

According to the static pressure cloud diagram, the static pressure distribution of the measuring pipe is basically the same, and the static pressure gradually decreases from the

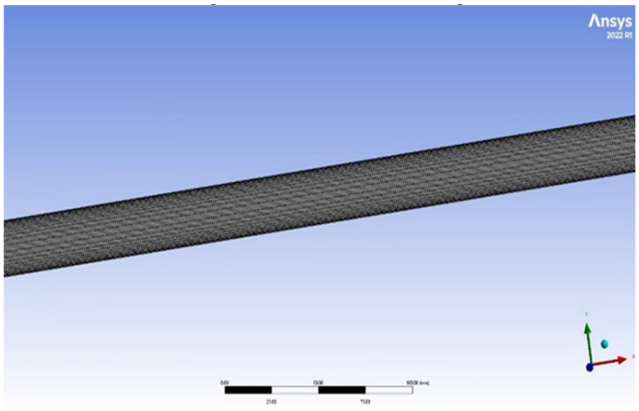

FIGURE 7. Grid diagram of measuring tube.

FIGURE 8. Simulated static pressure cloud image.

inlet to the outlet. Since no pressure is applied at the outlet of the simulated pipe, it tends to the atmospheric pressure. It can be seen from the tabular data and the graph that there is a large difference in the measured values of pressure difference under different viscosity, and the measured values of pressure difference increase with the increase of viscosity, which is conducive to improving the accuracy of pipeline viscosity measurement.

Simulation differential pressure data are shown in the table,

TABLE 1. Simulation differential pressure data sheet.

Viscosity (mPa·s)	40	80	120
Measuring point pressure difference (Pa)	1833.8	3475.3	5172.5

Figure 9 shows the simulation pressure diagram,

As can be seen from the simulated pressure curve in the figure above, the static pressure distribution in the pipeline gradually decreases with the increase of the distance from the inlet, and the greater the viscosity of the simulated fluid, the greater the pressure in the pipeline.

Similarly, the influence of different density and flow rate on measuring pressure difference is studied. Considering the different densities, the gravity was set as Y-axis -9.8m/s^2, the flow rate was 0.8m/s, and the kinematic viscosity was 0.05kg/(m·s). The SSTk-omega turbulence model was adopted.

Simulation differential pressure data are shown in the table,

Figure 10 shows the simulated static pressure cloud image:

Figure 11 shows the simulation pressure diagram,

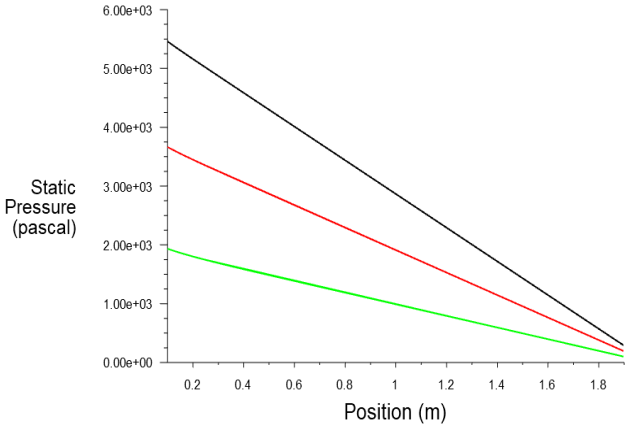

FIGURE 9. Simulated pressure curves.

TABLE 2. Simulation differential pressure data sheet.

Density (g/m³)	1.2	1.6	2.1
Measuring point pressure difference (Pa)	1835.8	2032.2	2247.9

FIGURE 10. Simulated static pressure cloud image.

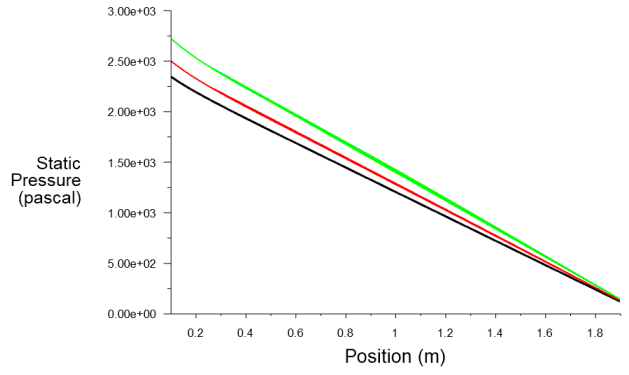

FIGURE 11. Simulated pressure curves.

The distribution of static pressure cloud map still shows a trend from large to small with the increase of the distance of the inlet, and the change of density has little influence on the measured value of pressure difference, but it is still needed under the requirements of high-precision measurement.

Similarly, considering the gravity as Y-axis -9.8m/s^2, density as 1100kg/m^3 and kinematic viscosity as 0.05kg/(m·s) for different flow rates, SSTk-omega turbulence model was adopted.

The inlet velocity cloud diagram is shown in Figure 12. As can be seen from the diagram, due to the presence of Bernoulli effect, the inlet velocity gradually increases from the pipe wall to the center point of the pipe, and the maximum velocity is greater than the corresponding inlet velocity. The boundary layer velocity at the pipe wall approaches zero, and the velocity stratification is obvious and tends to be stable after the inlet transition stage. Due to the limited size of the image, only the inlet part of the measuring tube was captured.

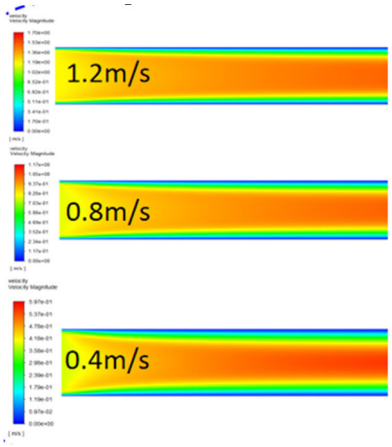

FIGURE 12. Simulated inlet velocity cloud image.

Simulation differential pressure data are shown in the table,

TABLE 3. Simulation differential pressure data sheet.

Flow rate (m/s)	1.2	0.8	0.4
Measuring point pressure difference (Pa)	3586.5	1834.7	1081.3

The simulation pressure curve is shown as follows,

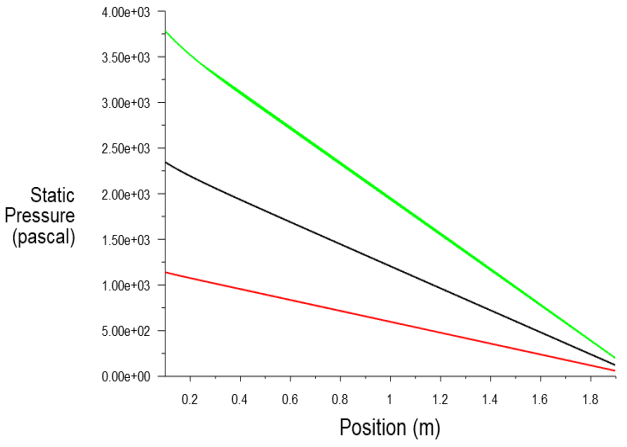

FIGURE 13. Simulated pressure curves.

It can be seen from the chart that under different velocity gradients, the pressure distribution in the pipe is basically the same, but the pressure difference is quite different, indicating that the inlet velocity has a great influence on the pressure measurement in the measuring pipe, and the pressure difference increases significantly with the increase of the flow rate.

B. SIMULATION OF MEASURING TUBES WITHOUT PULSATION

According to the analysis of the working principle of the diaphragm pump, the outlet flow rate of the diaphragm pump is sine wave pulsation, and the expression of the initial inlet speed is set as

$$inlet\_v = v * 1[m/s] * abs(\sin(2 * PI * f * t/1[s])) \quad (14)$$

The other conditions are the same as the simulation initialization parameters in the ideal state in the above section. The following diagram shows the change of inlet fluid velocity with time within 2s after setting at 0.8m/s pulsation,

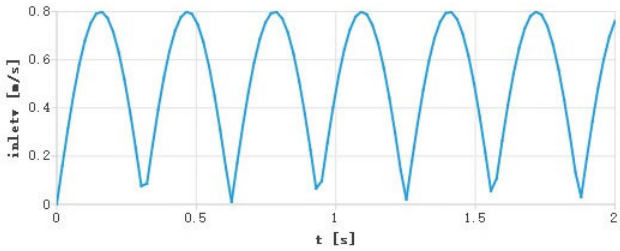

FIGURE 14. Fluent simulated inlet flow rate diagram in 2s.

Figure 16 shows the simulated static pressure cloud image when the simulation runs to the maximum pulsation speed. As can be seen from the figure, with the increase of the inlet inlet fluid flow rate, the outlet pressure gradually increases, and the inlet to outlet pressure gradually decreases. And the higher the initial flow rate at the inlet, the higher the flow rate at the same position in the pipeline.

Inlet velocity cloud diagram Figure 16,

It can be seen from the figure that the flow rate and pressure cloud pattern in the case of ideal constant current are consistent in the case of pulsation. The flow rate is lowest near the wall and the flow rate is highest in the center of the pipe.

As shown in Figure 18, when the pulsation frequency is 4.8Hz and the inlet flow rate is set to 0.4, 0.8, and 1.2m/s amplitude, the inlet pressure changes with time. According to the above pressure and time variation chart, it can be seen that the inlet pressure in the case of pulsating flow also changes periodically with the pulsation fluctuation.

As can be seen from the above simulation analysis results, in the case of non-pulsation and pulsation-based inlet velocity, in a certain one. At the point in time, the differential pressure distribution of the pipeline is also almost uniform. But there is a pressure turning point between 0∼0.2m, which is pulsationIf it is just in the interval of velocity change, the pressure of this section corresponds to the static pressure at the previous rate, so there may be a turning point of pressure, but the pressure before and after the turning point tends to changeThe potential is also a straight line.

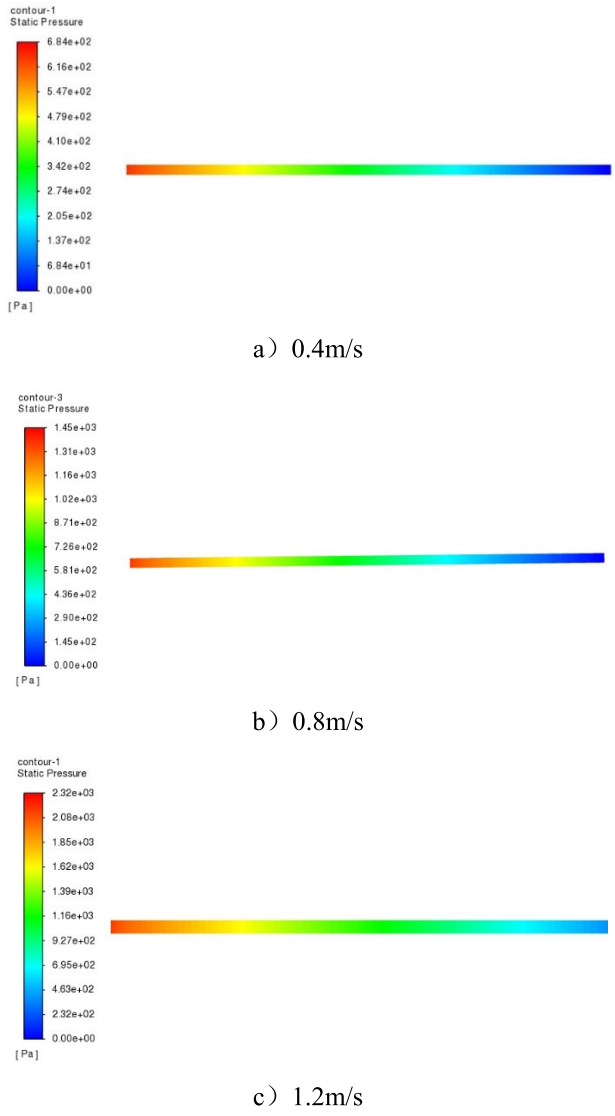

FIGURE 15. The static pressure cloud image is simulated under the pulsation of 0.4, 0.8 and 1.2m/s at 4.8Hz.

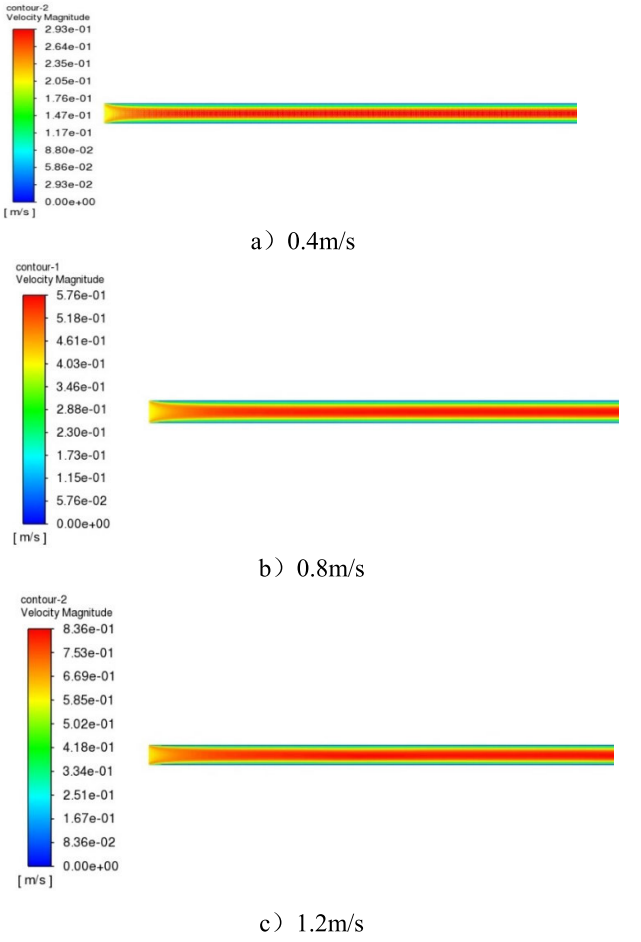

FIGURE 16. Tube velocity cloud image at 4.8Hz, 0.4, 0.8, 1.2m/s pulsation.

IV. RESEARCH ON MEASUREMENT SIMULATION AND CORRECTION MODEL OF STRAIGHT TUBE UNDER PULSATING FLOW

A. ERROR ANALYSIS OF STRAIGHT TUBE MEASUREMENT UNDER PULSATING CURRENT

Flow is measured by Coriolis mass flowmeter, whose forced vibration frequency ranges from 80Hz to 110Hz, while the diaphragm pump driving frequency set in this study is a maximum of 4.8Hz, that is, the maximum pulsation frequency of the fluid in the pipeline is 4.8Hz, which is only 0.1 times of the difference from 40Hz, so the impact of this deviation is ignored.

Differential pressure is measured using a capacitive differential pressure sensor, the measurement value is linearly related to the difference of the measured pressure at both ends, which is transmitted from the probe installed at different positions of the measuring tube through the silicone oil filling fluid to the central diaphragm. Therefore, when the fluid pulsation phenomenon occurs in the measuring tube, the difference in pressure measured by the center diaphragm of the sensor will also change. The production material of the central measurement diaphragm is generally engineering plastic. Here, it is taken as an example. Suppose to take a circular diaphragm, the material density is 1.45g/cm^3, the Young's modulus is 12GPa, the stiffness coefficient is 1.4N/mm, and the diaphragm mass is 10g. Then the first natural frequency of the diaphragm can be calculated,

$$f_1 = \frac{1}{2\pi}\sqrt{\frac{K}{m}} \tag{15}$$

where, f_1 is the first-order natural frequency of the diaphragm; K diaphragm stiffness coefficient, m diaphragm mass.

Through formula (15), it can be calculated that the first-order fixed frequency of the diaphragm is 56.8Hz, and it is known that the maximum operating frequency of one cylinder set by the diaphragm pump is 2.4Hz, and when the double-cylinder single-acting diaphragm pump works, the two pumps take turns, then the maximum operating frequency

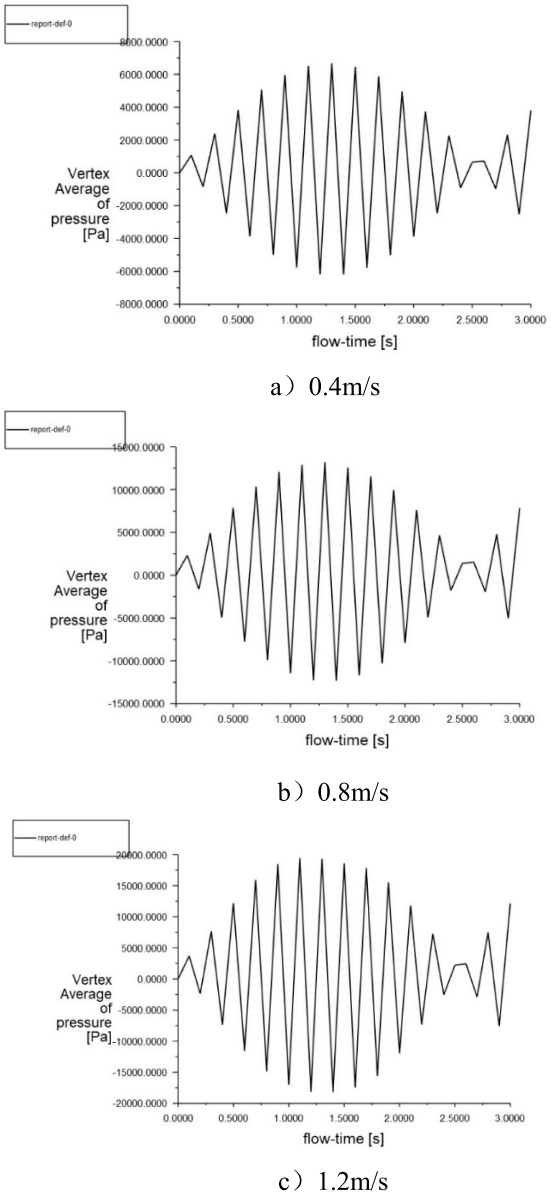

FIGURE 17. At 4.8Hz, 0.4, 0.8, 1.2m/s pulsation, the average pressure time line diagram of the inlet.

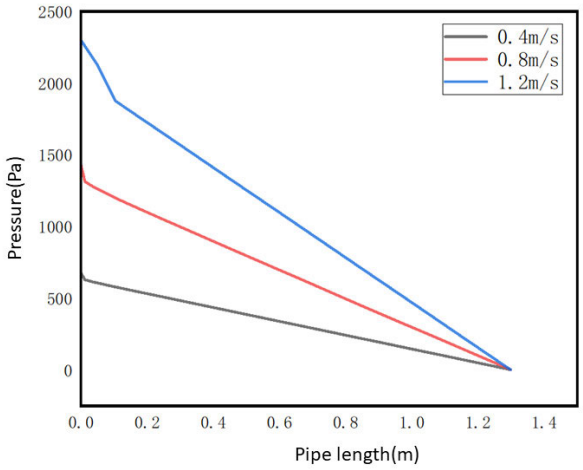

FIGURE 18. Diagram of variation of pressure difference in pipeline at different flow rates.

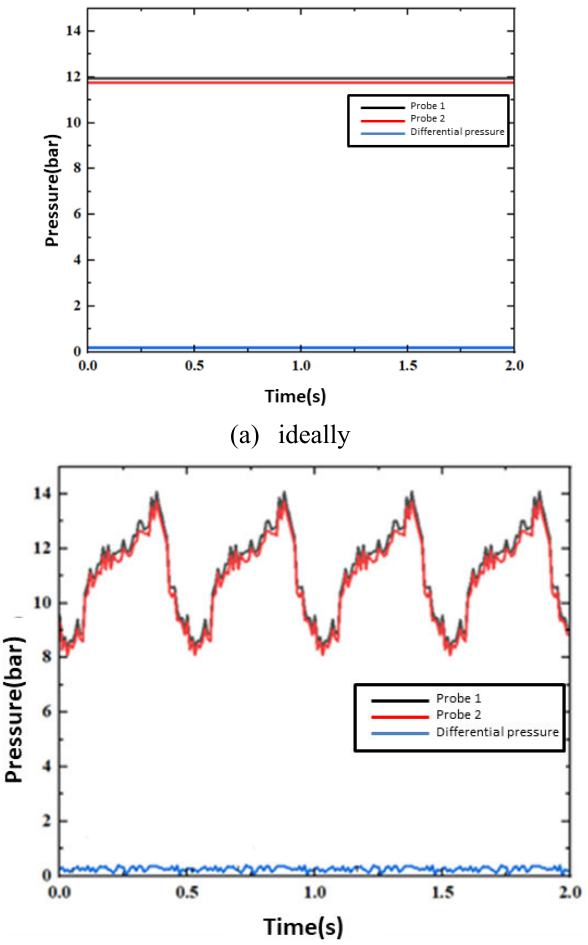

FIGURE 19. Numerical variation of pressure difference under fluid pulsation.

of the double cylinder is 4.8Hz. It is also very different from the calculated first-order natural frequency of the diaphragm, so the measurement error of the differential pressure sensor due to resonance is not considered.

The simulation results of the upper section pulsation flow down the measuring tube are compared and analyzed. Under ideal condition, the pressure difference values measured by the two probes are constant. However, in the case of pulsating flow caused by diaphragm pump, the inlet flow rate changes periodically with time, and the pressure difference value of the measuring pipe section also fluctuates, as shown in Figure 19. It can be seen that in the ideal state of constant flow, the pressure difference data in the tube is a horizontal line without any fluctuation, while in the case of pulsating flow, the pressure difference data in the tube constantly fluctuates with the fluctuation.

According to the simulation results in the previous section, the relative maximum deviation and relative average deviation between the pressure difference data of the diaphragm pump and the ideal value under different driving frequencies can be obtained, as shown in Figure 20.

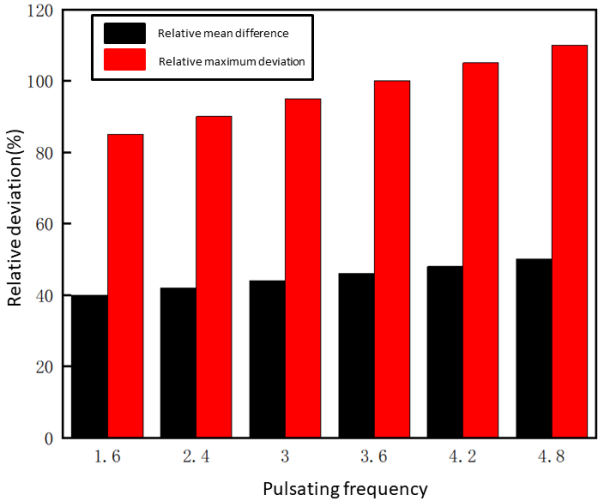

FIGURE 20. Relative deviation of pressure difference value under different driving frequency of diaphragm pump.

The maximum and average deviations of differential pressure data under different driving frequencies of diaphragm pumps are shown in Table 4,

TABLE 4. Differential pressure deviation of diaphragm pump under different driving frequency.

Drive Frequency (Hz)	4.8	4.2	3.6	3.0	2.4	1.6
Average deviation (bar)	0.251	0.211	0.164	0.127	0.091	0.058
Maximum deviation (bar)	0.296	0.282	0.253	0.206	0.142	0.09

It can be seen that the greater the driving frequency, the smaller the average deviation and the maximum deviation. What can be obtained from the data is that under actual measurement, the two probes are affected differently by complex ambient noise at different spatial positions, so the pressure difference deviation value will also be affected by other noises in the environment where the probe is located.

B. SIMULATION ANALYSIS OF ACTUAL MEASURING TUBE

Through the theoretical analysis of the characteristics of pulsating flow generated by diaphragm pump and the 2D model simulation analysis of measuring tube in Section III.B, it is concluded that the factors affecting the online measurement of linear rheology under pulsating current mainly lie in the impact on the pressure difference measurement. Therefore, the influence is small and the average flow rate over a period of time is used in the calculation of rheological parameters, so the influence of pulsating flow on the measured data of mass flow can be ignored. The following is the 3D model diagram of the measuring tube connecting section of the actual measuring device after grid division, as shown in Figure 21.

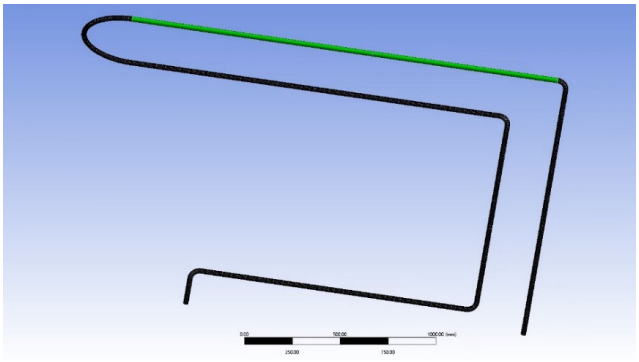

FIGURE 21. 3D model of the actual measuring tube mesh.

Since the pipe segment that actually plays a measuring role in the pipeline is the segment between the two probes of the differential pressure sensor, that is, the segment marked green in the above figure, the model of this segment is also used for simulation in our actual analysis. The installation distance between the two probes is 1.3m, and the inner diameter of the pipeline is 25mm.

Under the straight pipe measurement principle, the calculation of wall shear rate and shear stress can only be applied to the calculation model when the flow state of drilling fluid is laminar flow. Therefore, the flow pattern of drilling fluid in the measuring tube is judged, and the judging basis is Reynolds number. Its calculation formula is as follows,

$$Re = \frac{\rho D_h v}{\mu} \tag{16}$$

where, D_h is the inner diameter of the pipe, v fluid flow rate, μ fluid viscosity, ρ Fluid density in pipe.

The rheological parameters of initially configured oil-based drilling fluid samples were used for simulation and initial parameters were configured. Firstly, fluent was used for simulation analysis of pipeline flow rate. The minimum empirical value of viscosity set in this simulation analysis was 20mPa·s, and the maximum empirical value of density was 2500kg/m3.

In the figure above, the inlet of the measuring pipe section is at the lower bend. In actual measurement, when the setting voltage is 8V, the inlet speed is set as the maximum uniform flow rate of 0.861m/s, and the maximum flow rate under pulsation is 1.35m/s, which can be used to represent other conditions at lower speeds. Then the maximum flow rate is obtained as the simulation inlet flow rate, and then the change

of the flow rate in the whole pipe section of the measuring device is analyzed

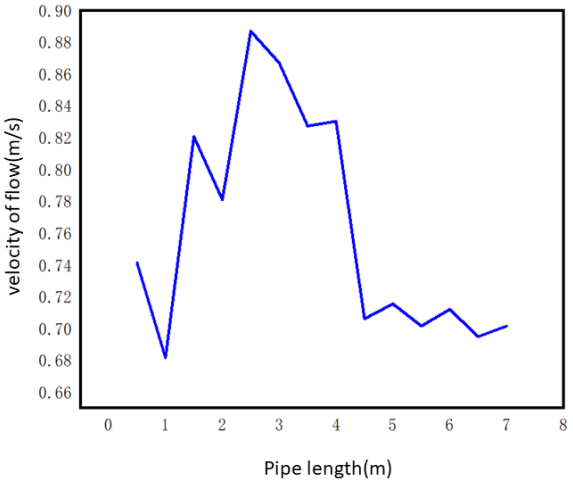

FIGURE 22. Flow rate line in pipe from inlet to outlet.

As can be seen from Figure 22, the fluid began to basically stabilize after the inlet pipe section reached the 4.5m pipe length. Moreover, it is the first thing to determine the flow pattern in the tube. It can be seen from equation (16) that density, viscosity, flow rate and pipe diameter are required to calculate Reynolds number. The designed experimental device has an inner diameter of 25mm and the maximum flow rate is constant. Therefore, it is only necessary to carry out simulation analysis in different actual density and viscosity ranges to obtain the fluid flow state in the measurement tube section of the experimental device.

As can be seen from Figure 23, when the viscosity is 20mPa.s, only the Reynolds number in the measuring pipe section with a density of 2500kg/m3 is greater than 2100 in the measuring pipe section with a density of 1∼4.5m. However, the measuring pipe section with a pressure difference sensor probe installed is 4.5∼6m, so the fluid flow in the measuring pipe section is laminar flow under the above fluid parameters. Therefore, the flow pattern is consistent with the calculation model of the shear rate of pipe wall, and the measurement calculation error caused by turbulence can not be considered in this experimental device.

The following is the original pressure diagram of the measuring tube section at the time of 2s with different pulsation velocity and amplitude.

Because this device uses a capacitive pressure difference sensor, the pressure data point extracted during simulation is static pressure, that is, the pressure acting on the wall is the most consistent with the actual measured pressure difference value. The following pressure value is the pressure value relative to atmospheric pressure (101325Pa). Table 5 shows the differential pressure data under different gradient voltages,

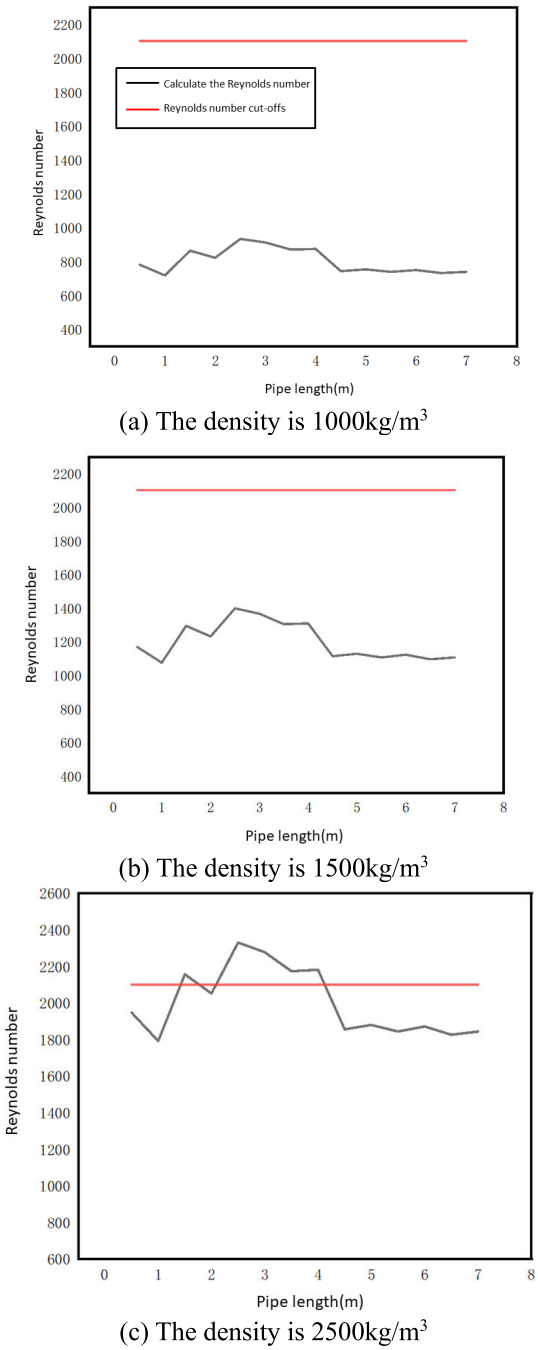

FIGURE 23. Reynolds number for different tube strengths at different densities.

C. THE MEASUREMENT CALIBRATION MODEL OF STRAIGHT TUBE UNDER PULSATING CURRENT IS ESTABLISHED

The pressure difference results of Fluent simulation were used to replace the standard experimental pressure difference data and establish the relationship with the parameters under different setting conditions, and the online measurement correction model was established for measuring the rheological properties of oil-based drilling fluids in a straight pipe under

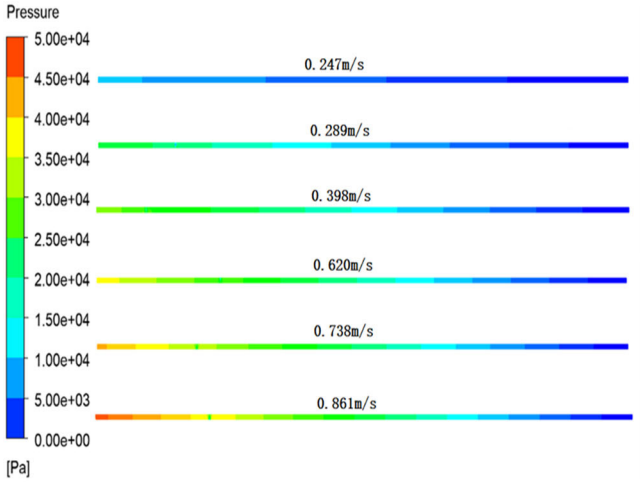

FIGURE 24. Cloud image of pipeline pressure at different flow rates.

TABLE 5. Pulsating current flow measurement tube simulation pressure difference value.

Pressure difference at 2V (Pa)	Pressure difference at 4V (Pa)	Pressure difference at 6V (Pa)	Pressure difference at 8V (Pa)
2630.56	16400	33100	60726.2
2550	15500	31100	56700
2184.6	13100	25800	46800
1600	9230	17900	32200
850	4460	8220	14300
9.9	-790	-2390	-5170
-839	-6010	-12800	-24200
-1610	-10700	-22100	-40900
-2220	-14300	-29100	-53700
-2620	-16500	-33300	-61100
2500	15700	32000	58900
2460	15100	30400	55600
2130	12800	25300	46000
1560	9020	17600	31600
820	4310	7930	13800
-13.9	-930	-2650	-5600
-858	-6130	-13100	-24600
-1630	-10800	-22200	-41300
-2240	-14400	-29300	-53900
-2630	-16500	-33400	-61300

pulsating flow. The measurement distance between the two probes of the sensor for measuring the pressure difference in the actual device is 1.3m, so the pressure loss of the fluid flowing in the pipeline is calculated according to a certain proportion. In the simulation, based on the flow gradient in Table 4-2, combined with the initial pulsating flow velocity at the inlet under the relationship between the driving voltage and the pumping frequency of the diaphragm pump, a large number of simulations were carried out under different viscosity and density conditions to obtain the pressure difference at the measurement tube. During the simulation, the fluid temperature was set at 25°C

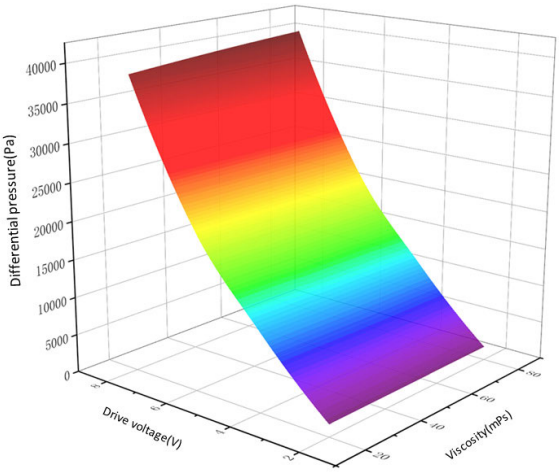

FIGURE 25. Profile of diaphragm pump driving voltage, viscosity and mean pressure difference under pulsating flow.

Figure 25 shows the three-dimensional surface diagram of the mean pressure difference of the measuring pipe segment obtained by the relative voltage and viscosity of different diaphragm pumps under pulsating current. The pressure difference value in the figure is the absolute average of the pressure difference in the measuring pipe section during one operating cycle of the diaphragm pump under the condition of pulsating flow. It can be seen that with the increase of driving voltage and viscosity, the average pressure difference of the measuring tube section also increases. The driving voltage is the X-axis value, the viscosity is the Y-axis value, and the pressure difference is the Z-axis. By surface fitting the data, the formula is as follows,

$$P_1 = 1 + 612.786x^2 + 21.491x + 0.353y^2 - 25.581y \tag{17}$$

Figure 26 shows a three-dimensional surface at constant current.

It can be seen from the surface diagram of the absolute mean pressure difference of the measuring tube section obtained at the pulsating current and the constant current pressure difference of the measuring tube section that the change trend of the two is basically the same. The following is a data fitting formula with constant flow.

$$P_2 = 1 + 600x^2 + 28.545x + 0.357y^2 - 25.745y \tag{18}$$

By using the pressure difference of the measuring tube section with constant current as the standard value and the average pressure difference of the pulsating current in one running cycle as the value under each pulsating gradient to fit close, the correction model of the measured pressure difference in the pulsating straight tube measurement can be

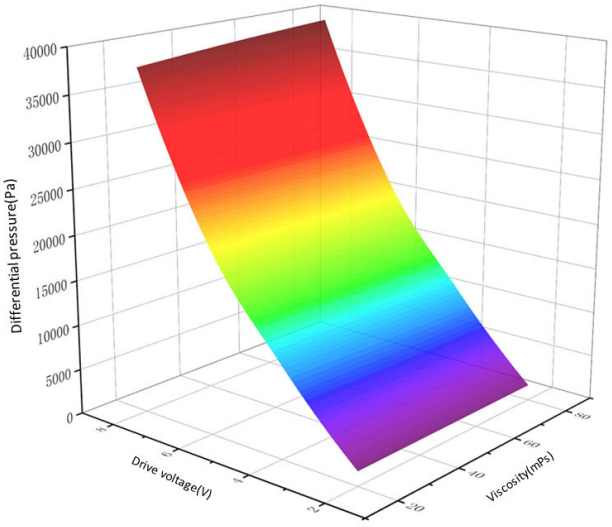

FIGURE 26. Constant current diaphragm pump driving voltage, viscosity and average pressure difference curve.

obtained as the difference between (17) and (18),

$$\Delta P_b = 12.786x^2 - 7.054x + 0.004y^2 - 0.164y \quad (19)$$

Finally, the measurement rheological correction model of the actual device is obtained from the fitting formula. In addition, only the data of the pumping cycle of a diaphragm pump is used in this paper for calculation and fitting during fitting. Therefore, the period of data collection of our actual experimental device is as long as it is an integer multiple of the pumping cycle of each driving voltage set, and then the average value of the measured pressure difference during this period is taken. The error caused by data acquisition can be greatly reduced.

V. EXPERIMENTAL VERIFICATION

A. EXPERIMENTAL PLATFORM CONSTRUCTION

Through the investigation and selection of the hardware required for the experimental frame, the hardware equipment of the device is installed and fixed in the processing and manufacturing. The external frame of the experiment, and then the circuit connection and debugging are carried out to complete the construction of the hardware experimental frame and determine the subsequent required simulation. Inlet boundary condition parameters. The experimental platform involves an electric double-cylinder single-acting diaphragm pump DBY3S-25AP316FFF, pneumatic tee. Ball valve Q641F25R, the heater is used to heat the pumped inlet oil-based drilling fluid, the temperature of the drilling fluid can be heated and controlled before flowing through the measurement system, the maximum temperature that can be heated is 80°C, the Coriolis mass flow meter model is DMF-1-U25, differential pressure sensing. The model is SN3851LT explosion-proof monocrystalline silicon micro-differential pressure transmitter, the measurement range is 0∼10MPa, and the accuracy is 0.25%F.S. The measuring tube is made of 25mm stainless steel round tube. The connection is flanged, and the outlet end of the electric diaphragm pump is stainless between the mass flow meter. Steel round pipe connection. The three-dimensional model of the overall installation of the experimental bench and the actual construction device are shown in Figure 27 and 28 below.

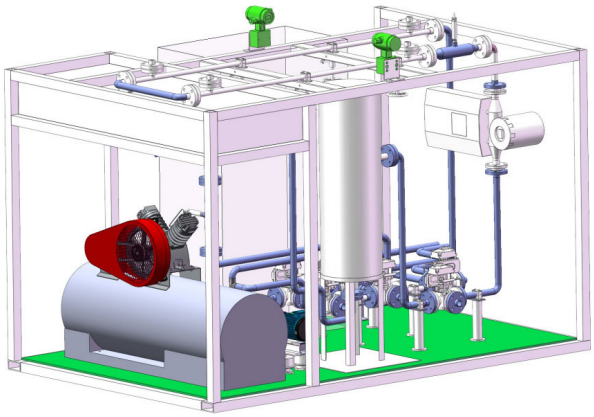

FIGURE 27. 3D model of the experimental stand.

FIGURE 28. The actual picture of the experimental frame.

B. ANALYSIS OF EXPERIMENTAL RESULTS

Through the experimental platform built, the experimental design of the factors that may affect the online rheological measurement of straight-pipe oil-base drilling fluid was carried out, and the experimental data were analyzed to find out the influence of each factor on the rheological measurement of straight-pipe oil-base drilling fluid based on pulsating flow. In the case of unstated, the test subject was the initial configuration of oil-based drilling fluid, and the measured temperature was 20°C, and the pressure was the pressure

generated during normal flow in the pipeline and was not pressurized.

The influence of flow velocity on the rheological measurement of the straight pipe drilling fluid is obtained by comparing the rheological measurement data of the straight pipe drilling fluid with that of the rotary viscometer.

The rheological curves of 2-4V and 4-8V were compared by several experiments to observe the measurement effect.

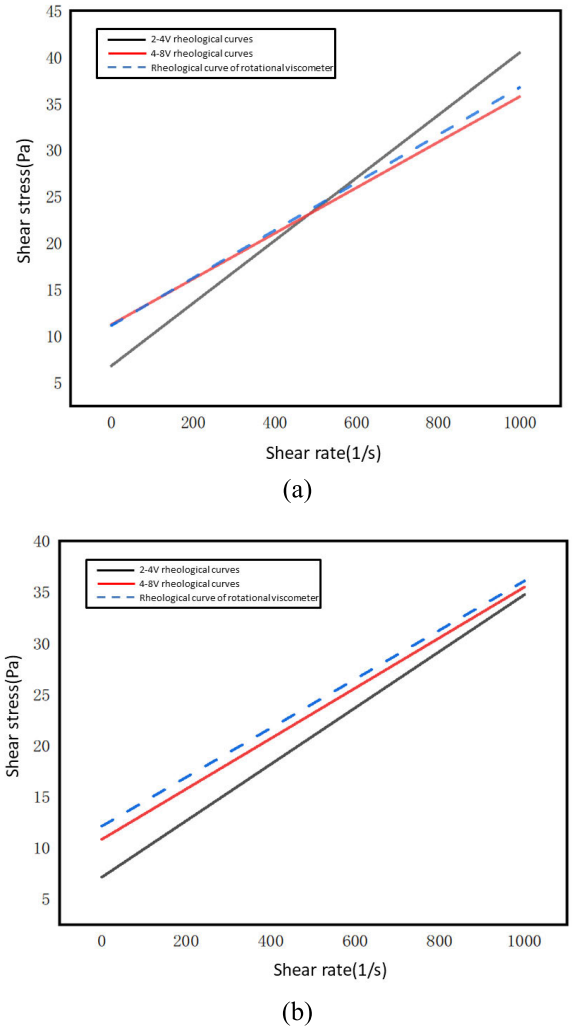

FIGURE 29. Comparison of two groups of rheological characteristic curves.

As can be seen from the comparison of rheological characteristic curves in figure 29, there is a large deviation between the voltage flow curve of the diaphragm pump set at 2-4V and that measured by the rotary viscometer at low flow velocity, which shows that the calculated plastic viscosity AV is too large and the dynamic shear force 0 is too small. However, the rheological characteristic curve at the diaphragm pump set at 4-8V almost coincides with that measured by the rotary viscometer at high flow velocity. It can be concluded that the rheological measurement accuracy of the straight pipe drilling fluid is better when the flow rate is larger.

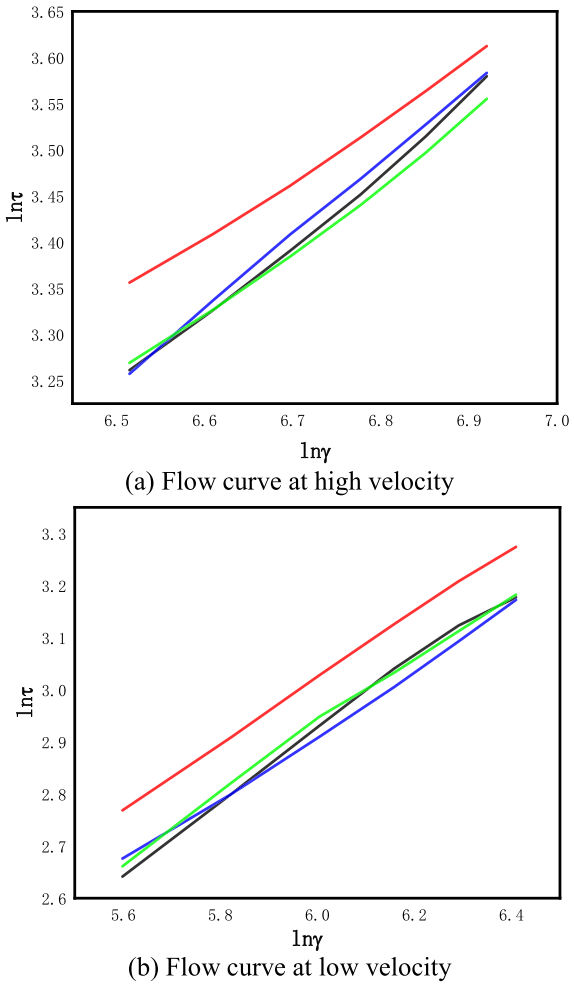

FIGURE 30. Flow curve at different velocity.

As can be seen from the comparison of flow curves in the figure, when the diaphragm pump voltage is set at 4-8V at a high flow rate, the flow curve calculated by the device has a good trend, while when the diaphragm pump voltage is set at 2-4V at a low flow rate, the flow curve trend is unstable, and the measurement effect is obviously poor

C. COMPARISON OF ACTUAL DRILLING FLUID MEASUREMENT DATA ON SITE

Five different viscosity oil-based drilling fluid samples were measured by experimental device and compared with manual measurement by rotary viscometer. The flow rate, pressure difference and density data collected by the experimental device are brought into the rheological model and correction model for calculation. Since the field generally focuses on the values of parameters such as plastic viscosity, apparent viscosity and dynamic shear force, the experimental results mainly analyze and compare these three parameters. The rheological curve calculated from the measured data is shown in figure 31

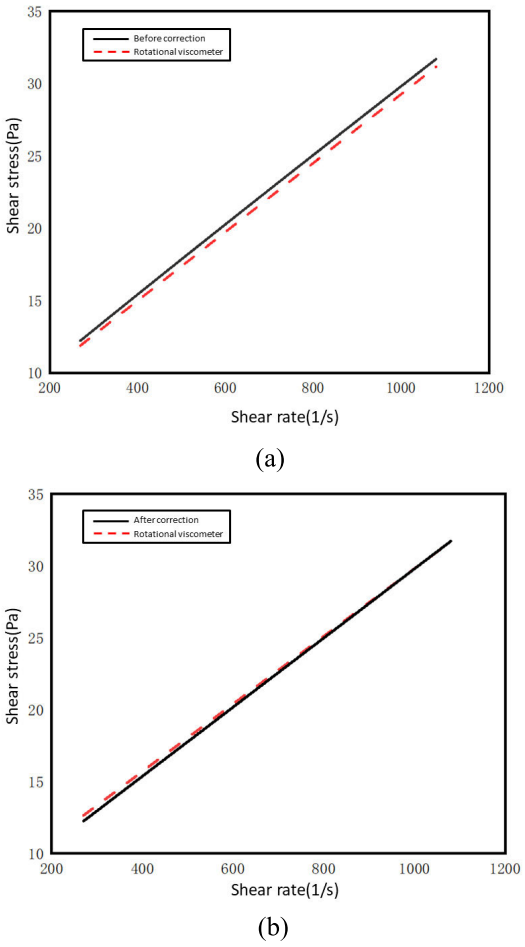

FIGURE 31. Comparison of data flow fitting curves before and after correction.

It can be seen that the trend of the fitted rheological curves after correction and the fitted curves measured by the rotational viscometer is basic close to coincident. The following is a comparison of the rheological parameters apparent viscosity (AV), plastic viscosity (PV) and dynamic shear force (YP) obtained by adding the measured data to the calibrated model and the measurement data of the rotational viscometer,

TABLE 6. Rheological parameters and deviation data sheet.

Experimental apparatus			Rotary viscometer			deviation		
AV	PV	YP	AV	PV	YP	AV	PV	YP
38.21	28.74	10.29	40	29.8	10.42	-1.79	-1.06	-0.13
43.78	32.54	13.12	45.25	32	13.54	-1.47	0.54	-0.42
53.3	40.46	13.06	52	39	13.29	1.3	1.46	-0.23
72.02	59.63	12.94	72	59	13.29	0.02	0.63	-0.35
89.36	70.73	19.22	92	72	20.44	-2.64	-1.27	-1.22

The average deviation of apparent viscosity (AV) is 2.69%, the average deviation of plastic viscosity (PV) is 2.362% and the average deviation of dynamic shear force (YP) is 3.056%. Compared with the original model without correction, the accuracy is greatly improved.

VI. CONCLUSION

This paper study a diaphragm pump for on-line rheological measurement of straight oil-based drilling fluids, which causes fluid pulsation and affects the rheological parameters of oil-based drilling fluids. Aiming to problem of low automatic measurement accuracy of drilling fluid rheology and the influence of fluid fluctuation flow, this paper proposes an online measurement method and correction method for the rheology of straight tubular oil-based drilling fluid under pulsating flow. Establish an online measurement model of rheology of straight tubular oil-based drilling fluid; The fluent is then used to drill the different rheological properties within the measuring tube. The fluid movement of the well fluid was simulated and analyzed, and then the error of the differential pressure measurement and flow measurement of the measuring pipe under the pulsating flow was analyzed. Will be real. The international measurement environment is used as the initialization parameter of the fluent simulation, and a large number of simulation calculations are carried out to obtain the simulation results, and the pulsation is established under the influence of pulsation. The device measures the correction model of oil-based drilling fluid, and finally obtains the correction by building an experimental platform and comparing the experimental data. The average deviation of the rheological parameters calculated by the post-model is 2.69% for apparent viscosity (AV) and 2.69% for plastic viscosity (PV). The average deviation of the yield point (YP) is 2.362%, which verifies that the model can improve the rheological measurement accuracy. In summary. The method proposed in this paper can measure the rheology of oil-based drilling fluid more accurately, and accurately measure the rheological performance. It provides theoretical support for the real-time monitoring of drilling fluid rheology in the actual drilling process.

REFERENCES

[1] R. L. Anderson, I. Ratcliffe, H. C. Greenwell, P. A. Williams, S. Cliffe, and P. V. Coveney, "Clay swelling—A challenge in the oilfield," *Earth-Sci. Rev.*, vol. 98, nos. 3–4, pp. 201–216, Feb. 2010.

[2] J. A. Andaverde, J. A. Wong-Loya, Y. Vargas-Tabares, and M. Robles, "A practical method for determining the rheology of drilling fluid," *J. Petroleum Sci. Eng.*, vol. 180, pp. 150–158, Sep. 2019.

[3] M. Gray and M. Miles. (2016). *Field Device To Measure Viscosity Density and Other Slurry Properties in Drilled Shafts: Final Report.* [Online]. Available: https://rosap.ntl.bts.gov/view/dot/31051

[4] J. Yin, J. Li, and Y. Xiao, "A new methodology of nonlinear parameter approximation used for rheological model of drilling fluids," in *Proc. 7th Int. Conf. Natural Comput.*, vol. 4, 2011, pp. 1919–1922.

[5] Y. Zhang, M. Huang, Y. Kan, L. Liu, X. Dai, G. Zheng, and Z. Zhang, "Influencing factors of viscosity measurement by rotational method," *Polym. Test.*, vol. 70, pp. 144–150, Sep. 2018.

[6] A. Saasen, T. H. Omland, S. Ekrene, J. Brévière, E. Villard, N. Kaageson-Loe, A. Tehrani, J. Cameron, M. Freeman, F. Growcock, A. Patrick, T. Stock, T. Jørgensen, F. Reinholt, H. E. F. Amundsen, A. Steele, and G. Meeten, "Automatic measurement of drilling fluid and drill-cuttings properties," *SPE Drilling Completion*, vol. 24, no. 4, pp. 611–625, Dec. 2009.

[7] N. Liu, H. Gao, Y. Xu, X. Chai, Y. Hu, and L. Duan, "Design and use of an online drilling fluid pipe viscometer," *Flow Meas. Instrum.*, vol. 87, Oct. 2022, Art. no. 102224.
[8] K.-I. Funakoshi and A. Nozawa, "Development of a method for measuring the density of liquid sulfur at high pressures using the falling-sphere technique," *Rev. Sci. Instrum.*, vol. 83, no. 10, Oct. 2012, Art. no. 103908.
[9] M. P. McIntyre, G. van Schoor, K. R. Uren, and C. P. Kloppers, "Modelling the pulsatile flow rate and pressure response of a roller-type peristaltic pump," *Sens. Actuators A, Phys.*, vol. 325, Jul. 2021, Art. no. 112708.
[10] O. E. Agwu, J. U. Akpabio, M. E. Ekpenyong, U. G. Inyang, D. E. Asuquo, I. J. Eyoh, and O. S. Adeoye, "A critical review of drilling mud rheological models," *J. Petroleum Sci. Eng.*, vol. 203, Aug. 2021, Art. no. 108659.
[11] R. Wiśniowski, K. Skrzypaszek, and T. Małachowski, "Selection of a suitable rheological model for drilling fluid using applied numerical methods," *Energies*, vol. 13, no. 12, p. 3192, Jun. 2020.
[12] S. D. C. Magalhães Filho, M. Folsta, E. V. N. Noronha, C. M. Scheid, and L. A. Calçada, "Study of continuous rheological measurements in drilling fluids," *Brazilian J. Chem. Eng.*, vol. 34, no. 3, pp. 775–788, Jul. 2017.
[13] B. S. Lee and E. I. Rivin, "Finite element analysis of load-deflection and creep characteristics of compressed rubber components for vibration control devices," *J. Mech. Des.*, vol. 118, no. 3, pp. 328–336, Sep. 1996.
[14] F. Lyu, S. Ye, J. Zhang, B. Xu, W. Huang, H. Xu, and X. Huang, "Theoretical and simulation investigations on flow ripple reduction of axial piston pumps using nonuniform distribution of pistons," *J. Dyn. Syst., Meas., Control*, vol. 143, no. 4, Apr. 2021, Art. no. 041008.
[15] M. G. Rabie, "On the application of oleo-pneumatic accumulators for the protection of hydraulic transmission lines against water hammer—A theoretical study," *Int. J. Fluid Power*, vol. 8, no. 1, pp. 39–49, Jan. 2007.
[16] P. Li, H.-A. Qiu, C. Wang, Y. Wu, and F. Miao, "Research on reverberation cancellation algorithm based on empirical mode decomposition," in *Proc. IEEE Int. Conf. Inf. Technol., Big Data Artif. Intell. (ICIBA)*, vol. 1, Nov. 2020, pp. 941–945.
[17] E. J. Garcia and J. F. Steffe, "Comparison of friction factor equations for non-newtonian fluids in pipe flow[1]," *J. Food Process Eng.*, vol. 9, no. 2, pp. 93–120, Apr. 1986.
[18] J. K. Zhang, G. S. Li, and Y. J. Guo, "Optimization and evaluation on drilling fluid rheological model," *Sci. Technol. Eng.*, vol. 13, no. 26, pp. 7619–7623, Sep. 2013.

XUEQIANG WANG received the master's degree from Southwest Petroleum University, China, in 2008. He is currently with the Engineering Technology Research Institute, PetroChina Southwest Oil and Gas Field Company. His research interest includes drilling engineering.

YILIN CHEN received the master's degree from Southwest Petroleum University, China, in 2018. He is currently with the Engineering Technology Research Institute, PetroChina Southwest Oil and Gas Field Company. His research interest includes petroleum.

WEN ZHANG received the bachelor's degree from Southwest Petroleum University, China, in 2009. He is currently with the Engineering Technology Research Institute, PetroChina Southwest Oil and Gas Field Company. His research interest includes drilling engineering.

JI ZHANG received the bachelor's degree from Southwest Petroleum University, China, in 2011. He is currently with the Engineering Technology Research Institute, PetroChina Southwest Oil and Gas Field Company. His research interest includes petroleum engineering.

YIN LEI received the master's degree from Southwest Petroleum University, China, in 2008. He is currently with the Engineering Technology Research Institute, PetroChina Southwest Oil and Gas Field Company. His research interest includes drilling engineering.

DONGXU TU received the bachelor's degree from Southwest Petroleum University, China, in 2009. He is currently with the Engineering Technology Research Institute, PetroChina Southwest Oil and Gas Field Company. His research interest includes drilling engineering.

HANG LU received the bachelor's degree from Yangtze University, China, in 2011. He is currently with the Engineering Technology Research Institute, PetroChina Southwest Oil and Gas Field Company. His research interest includes drilling engineering.

KE YAN received the master's degree from Southwest Petroleum University, in 2019. He is currently with the Exploration Division, PetroChina Southwest Oil and Gas Field Company. His research interest includes geological engineering.

GUOYONG XIA received the bachelor's degree from Chengdu University of Technology, China, in 2019. He is currently with the Development Department, PetroChina Southwest Oil and Gas Field Company. His research interest includes petroleum engineering.

HAOSEN YUAN received the bachelor's degree from Chongqing University of Science and Technology, in 2013. He is currently with the Engineering Technology Research Institute, PetroChina Southwest Oil and Gas Field Company. His research interest includes drilling engineering.

HAN ZHANG received the bachelor's degree from Chongqing University of Science and Technology, in 2014. He is currently with the Engineering Technology Research Institute, PetroChina Southwest Oil and Gas Field Company. His research interest includes drilling engineering.

YU XU received the master's degree from Chengdu University of Technology, in 2014. He is currently with the Engineering Technology Research Institute, PetroChina Southwest Oil and Gas Field Company. His research interest includes geological engineering.